Zoological Systematics, 45(4): 243–258 (October 2020), DOI: 10.11865/zs.202031

ORIGINAL ARTICLE

Phylogeography of *Gyrodactylus konovalovi* (Monogenoidea: Gyrodactylidae) in the Qinling Mountains in Central China

Tao Chen[1, 2], Xiaoning Chen[1], Biao Wang[1], Jianzhen Nie[1], Ping You[1 *]

[1]*College of Life Sciences, Shaanxi Normal University, Xi'an 710062, P.R. China*
[2]*Faculty of Basic Medical Sciences and Guangxi Key Laboratory of Diabetic Systems Medicine, Guilin Medical University, Guilin 541199, P.R. China*
[*]*Corresponding author, E-mail: youping@snnu.edu.cn*

Abstract *Gyrodactylus konovalovi* is an ectoparasite on the Amur minnow (*Rhynchocypris lagowskii*) that is widely distributed in the cold fresh waters of East Asia. In the present study, the phylogeography of *G. konovalovi* and the distribution of its host in the Qinling Mountains are examined. A total of 102 parasite specimens was sequenced for the mitochondrial cytochrome oxidase subunit 1 (*cox*1) gene, and 43 haplotypes were obtained. The ratio of substitution sites (dN/dS) was 0.016 and indicated strongly purifying selection. Haplotype diversity (h) and nucleotide diversity (π) of suprapopulations of *G. konovalovi* varied widely between distinct localities from the Qinling Mountains. Phylogenetic trees based on Bayesian inference (BI), maximum likelihood (ML) and maximum parsimony (MP) methods and network analysis revealed that all haplotypes were consistently well-supported in three different lineages A, B, and C, indicating a significant geographic distribution pattern. There was a significant positive correlation between genetic differentiation (Fst) and geographic distance ($P < 0.001$). The results of mismatch distribution, neutrality test and Bayesian skyline plot analyses showed that lineages A and B underwent population expansion after the Last Glacier Maximum (LGM) during the Late Pleistocene, while the lineage C underwent population contraction during the Middle to Late Pleistocene. Based on the molecular clock calibration, the most common ancestor was estimated to have emerged in the Middle to Late Pleistocene. Our study suggests that a clearly phylogeography of *G. konovalovi* was shaped by climatic oscillation and geological events, such as orogenesis, drainage capture changes and vicariance, during the Pleistocene in the Qinling Mountains in central China.

Key words *Gyrodactylus konovalovi*, Qinling Mountains, phylogeography, *cox*1, population expansion.

1 Introduction

Phylogeography is the study of historical processes that may be responsible for the contemporary geographic distributions of genealogical lineages within and among closely related species and is primarily conducted using molecular markers (Schneider, Cunningham & Moritz, 1998; Avise, 2000; Hansen, Bakke & Bachmann, 2007; Wu *et al.*, 2009; Li *et al.*, 2011; Wang *et al.*, 2012; Yu *et al.*, 2014; Pettersen *et al.*, 2015; Bowen *et al.*, 2016; Lumme *et al.*, 2016; Huang *et al.*, 2017; Huyse *et al.*, 2017; Hardouin *et al.*, 2018; Chen *et al.*, 2020). Phylogeography can be used to identify different historical forces, such as population expansion, population bottlenecks, climate oscillation, vicariance, and migration,

Received 16 April 2020, accepted 30 August 2020
Executive editor: Fuqiang Chen

analyze the variation in population distributions and reconstruct the evolutionary processes of fauna (Huang, 2012). Recently, animal mitochondrial DNA (mtDNA) permits an extension of phylogenetics referring to the microevolution between systematics and population genetics (Avise, 1987). Mitochondrial DNA is employed due to its maternal inheritance to trace maternal lineage far back in time, rapid mutation rate to track the ancestry of many species back hundreds of generations and the genetic relationships of specimens within species, and low level of intermolecular genetic recombination (Brown, George & Wilson, 1979; Giles *et al.*, 1980; Clayton, 1982).

The Gyrodactylidea includes a group of oviparous species from loricarid catfish in South America, and a group of viviparous species, which are found in bony fish, amphibians, crustaceans, and mollusks (Llewellyn, 1984; Boeger, Kritsky & Pie, 2003; Paetow *et al.*, 2009). More than 400 species have been described (Harris *et al.*, 2004), and specimens are found worldwide, parasitizing the skin, fins and gills of marine and freshwater fishes, both in the wild and captivity (Boeger, Kritsky & Pie, 2003; Bakke, Cable & Harris, 2007). Recently, three different genera (*Gyrodactylus* von Nordmann, 1832; *Paragyrodactylus* Gvosdev & Martechov, 1953; *Laminiscus* Palsson & Beverley-Burton, 1983) and sixty species of Gyrodactylidae Beneden & Hesse, 1864 were identified from freshwater fishes in China, including Cypriniformes, Gadiformes, Gasterosteiformes, Mugiliformes, Perciformes, Salmoniformes, and Siluriformes (Wu, Lang & Wang, 2000; Chen, 2018).

Gyrodactylus konovalovi Ergens, 1976 was described from specimens found on the fins, skin and gills of Amur minnow *Rhynchocypris lagowskii* Dybowski, 1869 from Mongolia and Russia (Ergens, 1976). Although the host *R. lagowskii* and related fish species were selected for phylogeographic studies due their widespread distributions in cold freshwater from the Lena and the Amur Rivers southward to the Yangtze drainages in East Asia (Min & Yang, 1986; Higuchi & Watanabe, 2005; Sakai *et al.*, 2014; Yu *et al.*, 2014; Hassan *et al.*, 2015; Xue *et al.*, 2017), there has limited study to be a corresponding study of *G. konovalovi* parasitzing *R. lagowskii* in the waters of the middle and eastern Qinling Mountains (Chen *et al.*, 2020). The Qinling Mountains have played important roles in influencing the phylogeography of a variety of organisms including *G. konovalovi*, *Feirana quadranus*, *Feirana taihangnica*, *Batrachuperus tibetanus*, *Pseudorasbora parva*, *Rhynchocypris oxycephalus*, and *Brachymystax lenok tsinlingensis* (Wang *et al.*, 2012., 2013; Yu *et al.*, 2014; Liu *et al.*, 2015; Huang *et al.*, 2017; Hardouin *et al.*, 2018; Chen *et al.*, 2020). These mountains represent a natural boundary between the northern and southern regions of the country and separate the Chinese temperate and subtropical climatic zones (Ding *et al.*, 2013), resulting in differentiated terrestrial and freshwater fauna (Li, 1981; Zhang, 1999). The split dates between *Pseudorasbora parva* and *G. konovalovi* are estimated to have occurred in the Middle Pleistocene and may have been a consequence of the rapid uplift (500–1500 m) of these mountains, which was influenced by the Qinghai-Tibet Plateau movement (Zhang & Fang, 2012; Hardouin *et al.*, 2018; Chen *et al.*, 2020). The Eurasian minnow *Phoxinus phoxinus* harbors the most diverse fauna of *Gyrodactylus* described on any fish species in the Palearctic Region, including seventeen species, whereas the Amur minnow *R. lagowskii* harbors three species of *Gyrodactylus* worldwide (Harris *et al.*, 2004). Therefore, *Gyrodactylus* species might be a suitable assembly for studying the ecology and phylogeographic evolution of a host-parasite system (Ziętara & Lumme, 2002). The generation time for gyrodactylids may be as short as two days (Bakke, Cable & Harris, 2007), which is considerably shorter than that of other taxa of monogeneans, may result in more rapid divergence at mitochondrial loci. Recently, there were some phylogeographic studies of species of *Gyrodactylus* in China and Europe, such as *G. konovalovi*, *G. salaris*, *G. arcuatus*, and *G. gondae* (Pettersen *et al.*, 2015; Lumme *et al.*, 2016; Huyse *et al.*, 2017; Chen *et al.*, 2020).

In the present study, the purpose is to use larger specimens data and wide geographical range in the Qinling Mountains to illustrate the distribution pattern of this parasite compared with previous study. Therefore, we examined the phylogeography of *G. konovalovi* based on the *cox*1 gene from 102 specimens from fifteen suprapopulations and its host distribution in the main Qinling Mountains. In addition, this study assessed the genetic differentiation between suprapopulations of parasites, demographic history, and the effects of geological events or climate oscillation during the Pleistocene on the current phylogeography of *G. konovalovi*.

2 Materials and methods

2.1 Ethics statement

This study was approved by the Animal Care and Use Committee of Shaanxi Normal University. The host species is not evaluated in the IUCN red list status (https://www.iucnredlist.org). None of the species (fish or parasite) sampled is endangered or protected in China (Yue & Chen, 1998). Host sampling is permitted by the local level authority in scientific research.

2.2 Sample collection

Specimens of *R. lagowskii* were sampled from 48 localities, which covered the most regions of the Qinling Mountains from May to October in 2016 and 2017. Fish were rapidly euthanized by a blow to the head and stored in 96% ethanol within three minutes. *Gyrodactylus* specimens were collected from the skin and fins of each host under a stereomicroscope in the laboratory, and one parasite specimen per host was used to avoid pseudoreplication because of viviparity (Bakke, Cable & Harris, 2007). Subsequently, specimens of *Gyrodactylus* were examined microscopically, and species identification was performed based on the morphology of the sclerotized structures of the haptor (Ergens, 1976; Chen *et al.*, 2020) and molecular ITS2 sequences (Ziętara & Lumme, 2002; Vanhove *et al.*, 2013). A total of 102 specimens of *G. konovalovi* from fifteen localities was identified (Fig. 1, Table 1). Finally, parasites and hosts were individually stored in 96% ethanol at 4°C. Voucher specimens of the parasites and hosts were deposited in the Fish Disease Laboratory, College of Life Sciences, Shaanxi Normal University, Xi'an, China, 710062 (Accession number: *R. lagowskii*: Acc.RL2017001–2017464 and *G. konovalovi*: Acc. GK2017001–2017102).

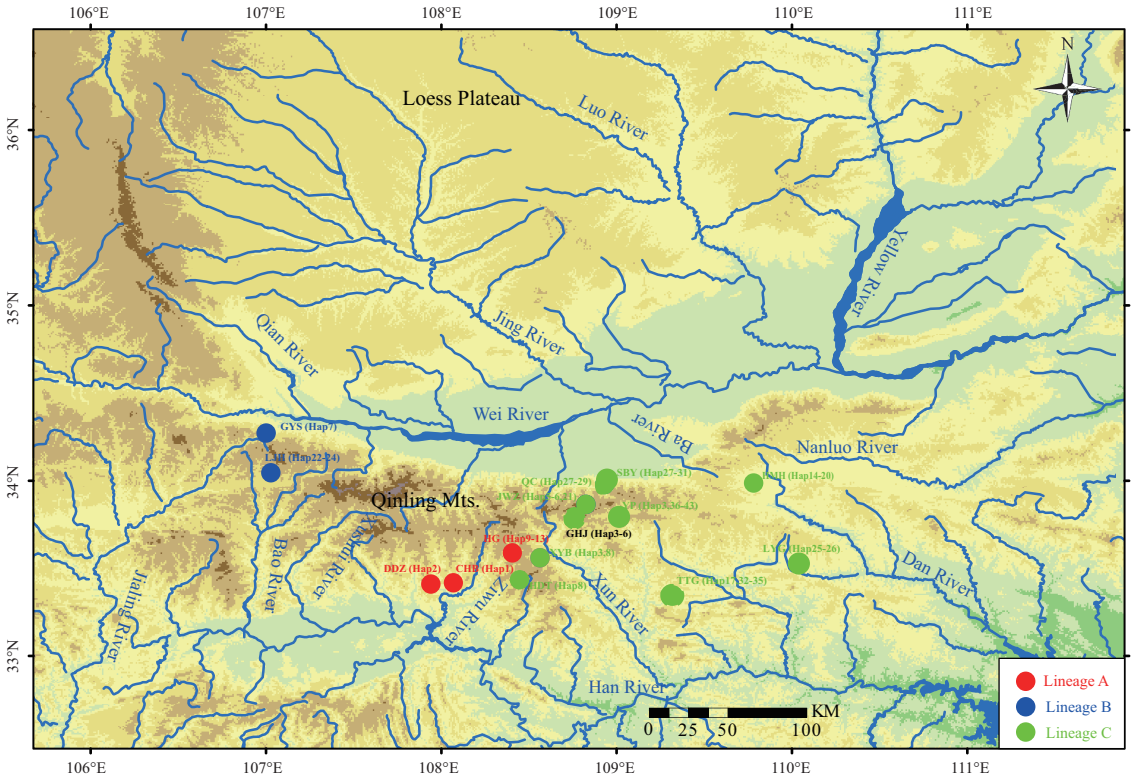

Figure 1. Map of sampling localities for *G. konovalovi* populations. The map was downloaded from the National Geomatics Center of China with slight modification using Arcgis10.1. The locality codes are given in Table 1. The lineages labeled red, blue, and green represent for lineages A, B, and C, respectively.

2.3 DNA extraction, PCR amplification and direct sequencing

Total genomic DNA of *Gyrodactylus* was extracted from each specimen following the same method described by Ye *et al.* (2017). A fragment of 518 bp of the Internal Transcribed Spacer 2 (*ITS2*) was amplified and sequenced for molecular identification of parasite specimens (You *et al.*, 2014). Fragments of the *cox1* gene were amplified by polymerase chain reaction (PCR) for 102 specimens of *G. konovalovi* from 15 suprapopulations using a new pair of primers designed based on the congeneric species *G. brachymystacis* and *G. parvae* (Ye *et al.*, 2017). The forward primer gkcox1-F (5'-TAAAGTGGGTAATATAGGAAAA-3') and the reverse primer gkcox1-R (5'-CTAAAGAGAAGACATAGTGGAA-3') were used to amplify a fragment of 536 bp of the *cox1* gene. Each PCR amplification was performed in a total volume of 25μl, containing 3 mM $MgCl_2$, 10 mM Tris-HCl (pH 8.3), 50 mM KCl, 0.25 mM of each dNTP, 1.25 U rTaq polymerase (TaKaRa, Dalian, China), 0.4 μM of each primer, 45 ng gDNA, tapped with Milli-Q water. The following cycling conditions were applied: initial denaturation for 1 min at 93°C followed by 35 cycles of denaturation for 10 s at 92°C, annealing for

Table 1. Sampling information and haplotype diversity based on the cox1 gene for fifteen suprapopulations of *Gyrodactylus konovalovi*.*

SC	Locality	Lineage	N	*Coordinates*	Elevation	Haplotypes	*h*	π
DDZ	Foping Co., Shaanxi Prov.	A	4	33.410476°N, 107.940753°E	964.5 m	Hap2(4)	-	-
CHB	Foping Co., Shaanxi Prov.	A	3	33.417045°N, 108.069953°E	665.4 m	Hap1(3)	-	-
HG	Ningshan Co., Shaanxi Prov.	A	6	33.587632°N, 108.406290°E	1315.5 m	Hap9(1), Hap10(1), Hap11(1), Hap12(2), Hap13(1)	0.933±0.122	0.00359±0.00080
LJH	Feng Co., Shaanxi Prov.	B	5	34.045245°N, 107.027867°E	1381.6 m	Hap22(3), Hap23(1), Hap24(1)	0.700±0.218	0.00855±0.00250
GYS	Weibin Co., Shaanxi Prov.	B	4	34.271956°N, 107.001503°E	892.0 m	Hap7(4)	-	-
HMH	Shangzhou Co., Shaanxi Prov.	C	8	33.986237°N, 109.781073°E	843.4 m	Hap14(1), Hap15(2), Hap16(1), Hap17(1), Hap18(1), Hap19(1), Hap20(1)	0.964±0.077	0.00358±0.00058
LYG	Shanyang Co., Shaanxi Prov.	C	5	33.526551°N, 110.039283°E	830.7 m	Hap25(4), Hap26(1)	0.400±0.237	0.00074±0.00044
JWZ	Chang'an Co., Shaanxi Prov.	C	9	33.864368°N, 108.824842°E	1685.1 m	Hap5(1), Hap6(7), Hap21(1)	0.417±0.191	0.00439±0.00210
QC	Chang'an Co., Shaanxi Prov.	C	5	33.977764°N, 108.932698°E	794.6 m	Hap27(2), Hap28(2), Hap29(1)	0.800±0.164	0.00223±0.00050
SBY	Chang'an Co., Shaanxi Prov.	C	9	34.005723°N, 108.946291°E	625.4 m	Hap27(1), Hap28(4), Hap29(2), Hap30(1), Hap31(1)	0.806±0.120	0.00403±0.00137
GHJ	Ningshan Co., Shaanxi Prov.	C	8	33.773644°N, 108.769971°E	1412.0 m	Hap3(1), Hap4(4), Hap5(2), Hap6(1)	0.750±0.139	0.01042±0.00258
YP	Zhashui Co., Shaanxi Prov.	C	10	33.784181°N, 109.035646°E	1106.2 m	Hap3(1), Hap36(1), Hap37(2), Hap38(1), Hap39(1), Hap40(1), Hap41(1), Hap42(1), Hap43(1)	0.978±0.054	0.00987±0.00190
TTG	Zhen'an Co., Shaanxi Prov.	C	10	33.363943°N, 109.304154°E	1053.1 m	Hap17(2), Hap32(5), Hap33(1), Hap34(1), Hap35(1)	0.756±0.130	0.01698±0.00698
XYB	Ningshan Co., Shaanxi Prov.	C	9	33.559413°N, 108.563282°E	1384.3 m	Hap3(2), Hap8(7)	0.389±0.164	0.00072±0.00031
HDT	Ningshan Co., Shaanxi Prov.	C	7	33.434294°N, 108.445810°E	1529.1 m	Hap8(7)	-	-

*Abbreviations in title: SC—Suprapopulations code; N—the number of individuals; *h*—haplotype diversity; π—nucleotide diversity.

1.5 min at 48°C and extension for 2 min at 60°C with a final extension for 6 min at 72°C. All PCR fragments were initially purified with a PCR purification kit (BGI Biotech, Shenzhen, China), subsequently subjected to electrophoresis in a 1% agarose gel and finally sequenced with PCR forward primer using an ABI Prism®3730 automated sequencer (Applied Biosystems, Foster City, USA).

2.4 Data analyses

2.4.1 Population genetic diversity

A total of 102 *cox1* gene sequences was visually inspected and manually edited using BioEdit v7.0.9.0 (Hall, 1999) and then aligned with MUSCLE (Edgar, 2004) as implemented in MEGA v6.06 (Tamura *et al.*, 2013). The nucleotide sequence compositions and the ratio of nonsynonymous (n) and synonymous (s) substitution sites (dN/dS) using maximum likelihood (ML) analysis of natural selection codon-by-codon by HyPhy were calculated in MEGA v6.06.

The molecular diversity indices for the number of haplotypes (H), haplotype diversity (h), and nucleotide diversity (π) were calculated in DnaSP v5.10.1 (Librado & Rozas, 2009). A substitution model for the haplotype dataset was determined using the Bayesian Information Criterion (BIC) in jModelTest v2.2.10 (Darriba *et al.*, 2012). The TIM3 model of molecular evolution with the gamma shape parameter and proportion of invariable sites (TIM3+I+G) was selected for the analysis of molecular variances (AMOVA) and phylogenetic analysis.

2.4.2 Phylogenetic and network analyses

Phylogenetic relationships based on the mitochondrial *cox*1 haplotypes were reconstructed using Bayesian inference (BI), maximum likelihood (ML), and maximum parsimony (MP) methods. The congeneric species *Gyrodactylus danastriae* Lumme, Ziętara & Lebedeva, 2017 and *G. parvae* You, Easy & Cone, 2008 were selected as outgroups (Lumme, Ziętara & Lebedeva, 2017; Ye *et al.*, 2017). Maximum parsimony analysis was implemented in PAUP 4.0b10a (Swofford, 2002). Heuristic searches with tree-bisection-reconnection were executed for 1,000 random addition replicates with all characters treated as unordered and equally weighted. Maximum likelihood analysis was conducted using RAxML v7.2.8 (Stamatakis, Ludwig & Meier, 2005), with bootstrap analysis performed with 1,000 replicates. Bayesian inference analysis was performed using MrBayes v3.1.2 (Ronquist & Huelsenbeck, 2003), and one set of four chains was allowed to run simultaneously for 10 million generations. The trees were sampled every 1,000 generations, with the first 25% being discarded as burn-in. Stationarity means that the log likelihood kept stable level with the sampled generations increasing, and it was considered to be reached when the average standard deviation of split frequencies was below 0.01. A haplotype network was then constructed using the median joining (MJ) network approach with MP Calculation in Network v5.0.1.1 (Bandelt, Forster & Röhl, 1999).

2.4.3 Population genetic structure

Genetic differentiation among populations was assessed using Fst pairwise differences. The molecular variance was partitioned among groups (Fct), among populations within groups (Fsc), and within populations (Fst) in Arlequin v3.5.1.2 (Excoffier & Lischer, 2010). The mean genetic distances among lineages were calculated by an uncorrected p-distance model in MEGA v6.06. In addition, the correlations between the genetic differentiation values of Fst and geographic distance of the sample localities were analyzed to test for isolation by distance (IBD) (Slatkin, 1993). The strength and significance of the relationships between genetic differentiation and geographic distance were assessed using linear regression in GraphPad Prism v 5.0 (www.graphpad.com).

2.4.4 Divergence time estimation

Divergence time estimation based on an uncorrelated lognormal relaxed molecular clock model was performed in BEAST v1.6.1 (Drummond & Rambaut, 2007). The divergence times of lineages were estimated using the TN93+I+G model and a Coalescent speciation tree prior because of the absence of fossil or geological data for calibration. The divergence rate of 7.2% per million years ago (Mya) was adopted, as it has been employed for mitochondrial gene analysis in *G. salaris* (Mieszkowska *et al.*, 2018). Analyses were performed using the same parameters described above for Bayesian inference. The estimates and convergence of effective sample size for all parameters larger than 200 were checked with Tracer v1.7.1 (Rambaut *et al.*, 2018). All resulting trees were then combined with LogCombiner v1.7.3 (Drummond & Rambaut, 2007).

A maximum credibility tree was then produced using TreeAnnotator v1.5.3 (Drummond & Rambaut, 2007) and visualized in FigTree v1.4.2 (Rambaut, 2014).

2.4.5 Demographic history

Three methods were used with the *cox*1 haplotype dataset to trace the demographic history of three lineages (A, B, and C). The neutrality test between Tajima's *D* (Tajima, 1989) and Fu's *Fs* (Fu & Li, 1993) was used to test for neutral evolution in Arlequin v3.5.1.2. The mismatch distribution was calculated in Arlequin v3.5.1.2 to test for signals of demographic expansion with a smooth unimodal curve (Harpending, 1994), and the significance of the sum of squared deviations (SSD) and Harpending's raggedness index (Hri) evaluated by bootstrap resampling (10,000 replicates). The beginning time of expansion (t) was calculated in accordance with a previous study (Lumme *et al.*, 2016). Bayesian skyline plot (BSP) analysis was applied in BEAST v1.6.1 to describe demographic history by assessing the time variation of effective population size. This analysis was performed using the TN93+I+G substitution model with a divergence rate of 7.2% per Mya and 10 million generations.

3 Results

3.1 Genetic diversity

The values of the mean distance of ITS2 sequences among fifteen localities of *Gyrodactylus* species were within the threshold of 1.39% (Vanhove *et al.*, 2013) (Table 2), then combined with morphology of sclerotized structures of the haptor, *Gyrodactylus* specimen was identified as *G. konovalovi*. A total of 102 sequences of *G. konovalovi* from 15 geographic localities was obtained (Fig. 1). The sequence alignment provided a dataset matrix of 536 bp, of which 115 bp (21.5%) were parsimony informative sites. Base frequency was biased with the AT content reaching 68.0%. A total of 43 haplotypes was identified (Table 1). The haplotypes exhibited distinct geographic distribution with 35 unique haplotypes (localities code: DDZ, CHB, HG, LJH, GYS, LYG) and 8 shared haplotypes (localities code: HMH, JWZ, QC, SBY, GHJ, YP, TTG, XYB, HDT). The ratio of substitution of nonsynonymous and synonymous sites (dN/dS) was 0.016, indicating strong purifying selection against nonsynonymous substitutions. All haplotype sequences were deposited in GenBank under accession numbers MN379691–MN379733.

Total haplotype diversity (h) and genetic diversity (π) across the samples were 0.962±0.009 and 0.06268±0.00598, respectively, indicating high level of genetic diversity. The h was highest in the YP population, whereas π was highest in the TTG population. The h and π were lowest in the XYB population, except for four localities (population code: CHB, DDZ, GYS and HDT), and the relationship between genetic diversity and the population latitude was uncorrelated (Table 1).

Table 2. Mean distance of ITS2 sequences between populations of *G. konovalovi*.

Code	CHB	DDZ	GHJ	GYS	HDT	HG	HMH	JWZ	LJH	LYG	QC	SBY	TTG	XYB	YP
CHB															
DDZ	0.000														
GHJ	0.010	0.010													
GYS	0.014	0.014	0.008												
HDT	0.010	0.010	0.000	0.008											
HG	0.000	0.000	0.010	0.014	0.010										
HMH	0.010	0.010	0.000	0.008	0.000	0.010									
JWZ	0.011	0.011	0.001	0.009	0.001	0.011	0.001								
LJH	0.014	0.014	0.008	0.000	0.008	0.014	0.008	0.009							
LYG	0.010	0.010	0.000	0.008	0.000	0.010	0.000	0.001	0.008						
QC	0.010	0.010	0.000	0.008	0.000	0.010	0.000	0.001	0.008	0.000					
SBY	0.010	0.010	0.000	0.008	0.000	0.010	0.000	0.001	0.008	0.000	0.000				
TTG	0.010	0.010	0.000	0.008	0.000	0.010	0.000	0.001	0.008	0.000	0.000	0.000			
XYB	0.010	0.010	0.000	0.008	0.000	0.010	0.000	0.001	0.008	0.000	0.000	0.000	0.000		
YP	0.010	0.010	0.000	0.008	0.000	0.010	0.000	0.001	0.008	0.000	0.000	0.000	0.000	0.000	

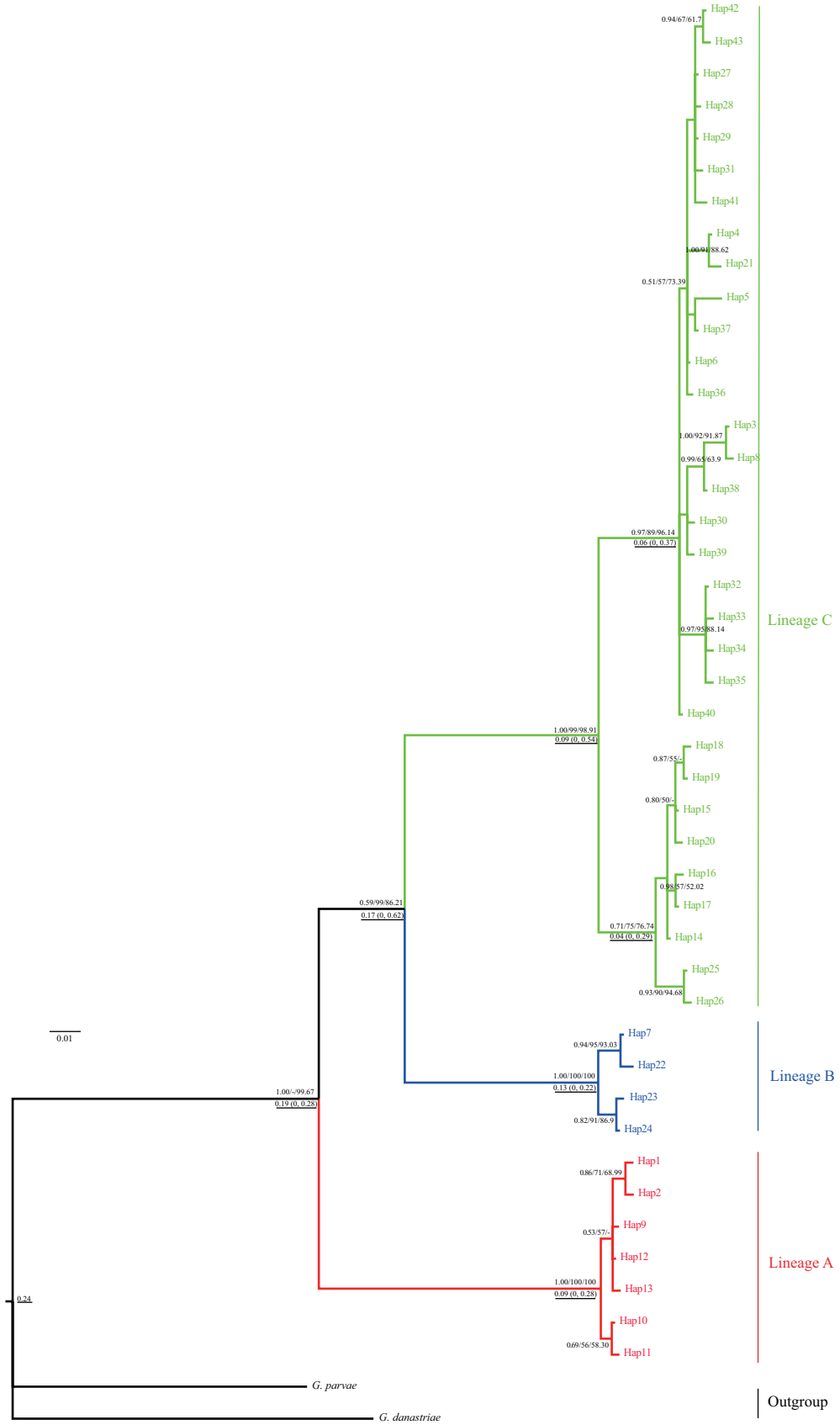

Figure 2. Bayesian inference tree of haplotypes based on *cox*1 sequences of *G. konovalovi*. The numbers above nodes are Bayesian posterior probabilities, maximum likelihood (ML) and maximum parsimony (MP) bootstrap values, respectively (those above 50% are shown). The three lineages are differentiated by different colors (red, Lineage A; blue, Lineage B; green, Lineage C). Estimated divergent dates in Mya are given in numbers down nodes with underline.

3.2 Phylogenetic and network analyses

The phylogenetic trees (BI, ML, and MP) based on the haplotype *cox1* sequences showed congruent topologies and were consistently divided into three lineages (the BI tree is shown in Fig. 2). Lineage A, at the base of the tree, was comprised of three localities (population code: CHB, DDZ, and HG) from the Han River tributaries in the middle Qinling Mountains. Lineage B, corresponding to two localities (population code: LJH and GYS) from the Han River and Wei River tributaries in watershed of the western Qinling Mountains. Lineage C, representing ten localities (population code: HMH, LYG, GHJ, YP, QC, SBY, JWZ, TTG, XYB, and HDT) from the Wei River and Han River tributaries in the middle and eastern Qinling Mountains, showing frequent gene flow between suprapopulations of *G. konovalovi* in the region of watershed because of drainage capture. This pattern corresponded to significant geographic distribution of lineages in the Qinling Mountains.

Network analysis revealed that all haplotypes of *cox1* sequences were consistently well-supported by three different lineages (Fig. 3), indicating a significant geographic distribution pattern. All unique haplotypes were connected in a reticulate manner. These relationships revealed a phylogeographic pattern of *G. konovalovi* in the Qinling Mountains.

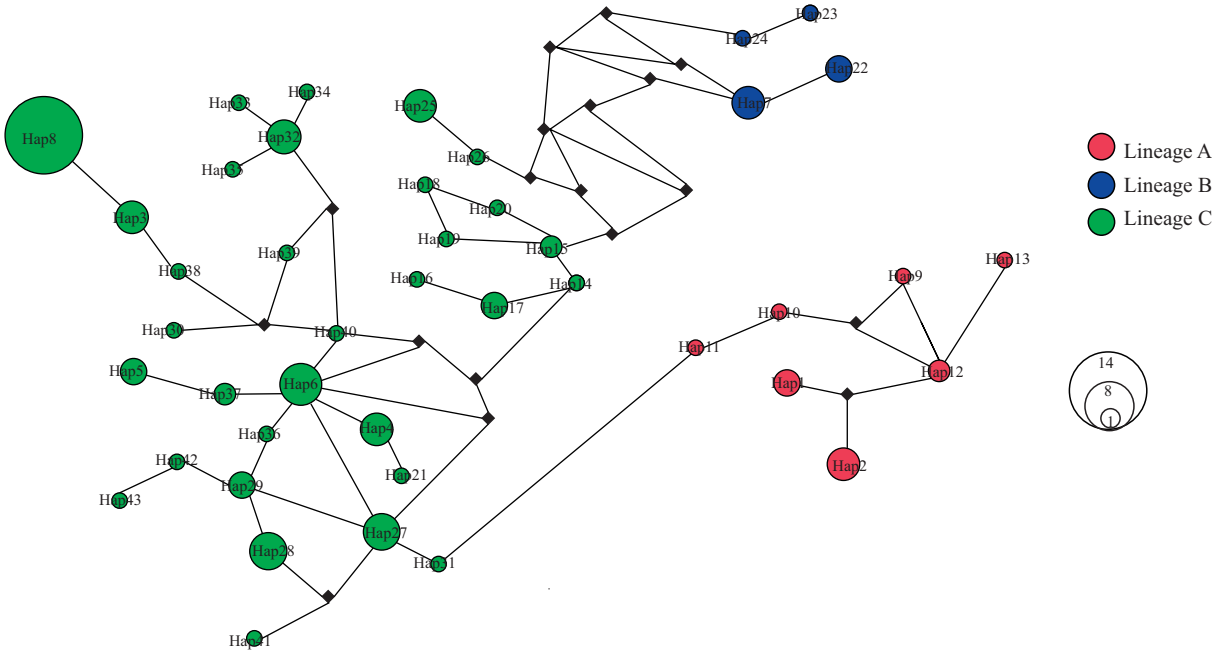

Figure 3. Median-joining network for all haplotypes of *G. konovalovi* based on the *cox*1 gene. The lineages colors correspond to Fig. 2.

3.3 Population genetic structure

Analysis of molecular variances (AMOVA) indicated a highly significant genetic differentiation among groups (83.31%), among populations (12.63%) and within populations (4.06%). The genetic differentiation metric Fst (0.95943) was very high within populations (Table 3). This pattern corresponded to the geographic structure and genetic differentiation value of Fst in the Qinling Mountains. Furthermore, there was a significant positive correlation between genetic differentiation (Fst) and geographic distance (R^2=0.2508, P<0.001) (Fig. 4).

3.4 Divergence time estimation

A molecular clock was estimated for the haplotypes of *cox*1 of *G. konovalovi* (Fig. 2). The time since the most recent common ancestor of the whole ingroup was dated to 0.24 Mya (95%HPD: 0–0.28 Mya). Lineage A diverged 0.19 Mya (95%HPD: 0–0.28 Mya), and lineage B and lineage C diverged 0.17 Mya (95%HPD: 0–0.62 Mya). All divergence times occurred during the Middle Pleistocene.

3.5 Demographic history

The neutrality test between Tajima's *D* values of all lineages was positive and Fu's *Fs* values of lineages A and C were

negative and non-significant (Table 4). However, the values of the SSD and Hri index of all lineages did not reject the hypothesis of sudden expansion and mismatch distribution of lineages A and B were unimodal, showing population expansion, while, lineage C was multimodal, rejecting population expansion and suggesting a stability (Fig. 5). The BSP suggested that the effective population size increased rapidly for all lineages of *G. konovalovi* approximately 0.015 Mya after the Last Glacier Maximum (LGM) during the Late Pleistocene, however, the lineage C underwent a steep decline after 0.15 Mya during the Middle to Late Pleistocene (Fig. 6). Therefore, all lineages were discordant in the demographic scenarios based on three methods. The results of the mismatch distribution, neutrality test and BSP analyses showed that the lineage C underwent contraction during the Middle to Late Pleistocene and lineages A and B underwent population expansion after the LGM during the Late Pleistocene.

Table 3. Results of hierarchical analysis of molecular variance (AMOVA) based on haplotypes of *G. konovalovi*.*

Source of variation	Degree of freedom	Sum of squares	Variance components	Percentage of variation	Fixation indices
Among groups	2	1163.397	30.27635 Va	83.31	Fct^{**} = 0.83310
Among populations	12	405.073	4.59106 Vb	12.63	Fsc^{**}= 0.75692
Within populations	87	128.275	1.47443 Vc	4.06	Fst^{**}= 0.95943
Total	101	1696.745	36.34183		

*Significant level: P^{**}<0.01.

Table 4. Statistics for genetic diversity, neutrality test, mismatch analysis and the time of the expansion based on lineages of *cox*1 haplotypes of *G. konovalovi*.*

Lineages	*h*	π	Hri	SSD	Tajima's *D*	Fu's *Fs*	tau	t (Mya)
Lineage A	0.872±0.067	0.00545±0.00069	0.04471	0.01014	0.51848	-1.17932	3.598	0.02331
Lineage B	0.750±0.112	0.00570±0.00200	0.18133	0.10306	0.17279	1.33669	8.344	0.05405
Lineage C	0.944±0.013	0.02379±0.00201	0.01167	0.02568	0.77652	-2.66141	6.191	0.03887
Total	0.962±0.009	0.06268±0.00598	0.01022	0.02818	1.50468	1.71627	24.000	0.15547

*Abbreviations in title: *h*—haplotype diversity; π—nucleotide diversity; Hri—harpending's raggedness index; SSD—sum of squared deviation; tau—expansion parameter; t—beginning a time of expansion; Mya—million years ago. Significant level: P^{*}<0.05, P^{**}<0.01.

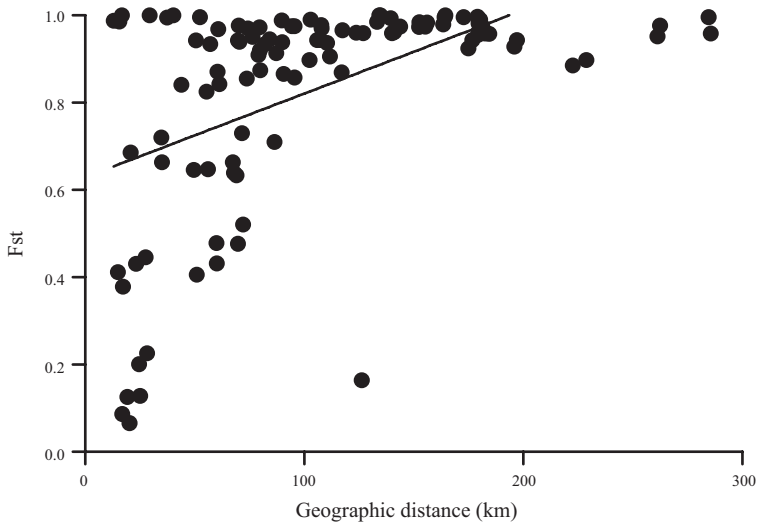

Figure 4. Plots of genetic differentiation estimates of Fst against geographic distance (km) between populations within the *cox*1 dataset of *G. konovalovi*. The linear regression overlays the scatter plots (R^2=0.2508, P<0.001).

4 Discussion

The molecular data of *G. konovalovi* showed high levels of genetic diversity, with the 35 unique haplotypes and 8

shared haplotypes more than the 18 unique haplotypes and 7 shared haplotypes of same parasite in previous study, indicating frequent gene flow adjacent to the watershed region because of some connectivity between the sampled rivers (Chen *et al.*, 2020). Vicariance and uplift promote genetic differentiation and fragmentation of subpopulations, which confirm that drainage capture accelerates freshwater fish distribution and dispersal (Zhang & Chen, 1997; Albert & Crampton, 2010; Zhang & Fang, 2012; Albert *et al.*, 2017). The gene flow of host-specific trematodes depends on the dispersal of the salmon host (Criscione & Blouin, 2004). Barriers to fish upstream migration will reduce the genetic exchange and result in isolation between parasite populations (Blasco-Costa, Waters & Poulin, 2012). The genetic diversity loss among populations with effective population size decline is suspected to be caused by genetic drift, bottleneck, founder effect, habitat fragmentation, inbreeding, and gene flow deficiency (Hunter & Gibbs, 2006).

In this study, the genetic diversity did not show a significant south to north decreasing trend among populations of *G. konovalovi* in accordance with observations on *F. quadranus, G. konovalovi*, and *R. oxycephalus* in the Qinling Mountains, and *G. arcuatus* and *G. gondae* in Europe (Wang *et al.*, 2012; Yu *et al.*, 2014; Lumme *et al.*, 2016; Huyse *et al.*, 2017; Chen *et al.*, 2020), indicating the existence of multiple refugia among the Qinling Mountains during the Last Glacial Maximum (LGM). In Europe and North America, *Tamias striatus* expanded from southern refugia after the LGM (Rowe *et al.*, 2004). The genetic diversity of these species is usually geographically structured with declines in genetic diversity towards the north (Hewitt, 1996). The genetic diversity of the marine parasite *Mazocraeoides gonialosae* also displayed a decreasing tendency from south to north along the coasts of the South and East China Seas (Li *et al.*, 2011). However, populations with high haplotype diversity and low nucleotide diversity of *M. gonialosae* and *G. salaris* and a star-shaped haplotype network are indicative of a classic postglacial expansion after a period of low effective population size, with rapid population growth enhancing the retention of new mutations, accumulating haplotype diversity, but lacking enough time to accumulate nucleotide diversity (Hewitt, 1996; Grant & Bowen, 1998; Li *et al.*, 2011; Pettersen *et al.*, 2015).

Gene flow was considerably higher in oviparous monogenean parasite *M. gonialosae* that was studied along the coasts of the South and East China Seas (Li *et al.*, 2011). While restricted gene flow and most unique haplotypes between the populations of *G. salaris* in the Glomma River in Norway and *G. konovalovi* in the middle and eastern Qinling Mountains might cause mutations to persist in isolated populations that have been separated for a long time (Mills, 2007; Pettersen *et al.*, 2015; Chen *et al.*, 2020). A small population might lead to a strong genetic drift, and the reduced genetic diversity due to bottleneck increased genetic drift might increase inbreeding and genetic homogeneity to decrease population fitness (Mills, 2007).

Divergence among haplotypes based on the *cox*1 gene of *G. konovalovi* ranging from 0.20% to 14.70% was clearly higher than that found in Monogenoidea parasites, such as *M. gonialosae* (0.01% to 2.08%), *G. salaris* (0.00% to 3.41%), *G. truttae* (0.10% to 0.50%), *G. teuchis* (0.10% to 11.00%), *G. konovalovi* (0.20% to 12.10%), and *G. corydori* (0.10% to 6.21%) (Meinilä *et al.*, 2002; Bueno-Silva, Boeger & Pie, 2011; Li *et al.*, 2011; Hahn *et al.*, 2015; Mieszkowska *et al.*, 2018; Chen *et al.*, 2020). These values of divergence among haplotypes sequence could represent a recent separation.

The substitution rate (dN/dS) was 0.016, indicating strong purifying selection with genes of relatively low nucleotide diversity (π) against nonsynonymous substitutions in accordance with results from other gyrodactylids based on *cox*1 and *ND*5 genes, such as *G. salaris*, *G. teuchis, G. arcuatus,* and *G. konovalovi* (Meinilä *et al.*, 2004; Pettersen *et al.*, 2015; Lumme *et al.*, 2016; Chen *et al.*, 2020). The ratio of substitution sites (dN/dS) of all the protein-coding genes below 0.1 indicates that each gene is subject to strong purifying selection, in which the biological functions of proteins are safeguarded against deleterious mutations (Huyse, Buchmann & Littlewood, 2008; Chen *et al.*, 2020); this feature is typical of mitochondrial protein-coding genes (Rand & Kann,1998). However, Bueno-Silva and Boeger (2019) amplified and sequenced fragments of the *COII* gene, not *COI*. Even so, you could compare your results to those obtained by Bueno-Silva and Boeger (2019). In addition, these authors found out that *COII* was evolving essentially under purifying selection, including some sites under positive selection. On the other hand, Bueno-Silva *et al.* (2011) amplified and sequenced fragments of the *COI* gene. These latter authors suggested that this gene was evolving under positive selection, which is likely associated with local adaptation of lineages of parasites (Bueno-Silva, Boeger & Pie, 2011; Bueno-Silva & Boeger, 2019).

The topologies of the phylogenetic trees and network analyses yielded similar results, both indicating well-supported three lineages, revealing a significant phylogeographic pattern of *G. konovalovi* in the Qinling Mountains (Chen *et al.*, 2020). The AMOVA indicated strong geographic structuring with significant genetic differentiation among and within populations. This pattern corresponds to a significantly geographic structure and genetic differentiation of *G. konovalovi* in the Qinling Mountains (Chen *et al.*, 2020).

The Qinling Mountains have played an important role in the phylogeography of parasite, amphibian, and fish species, which may have led to the fragmentation of populations by vicariance (Wang *et al.*, 2012; Wang *et al.*, 2013; Meng, Li &

Qiao, 2014; Yu *et al.*, 2014; Liu et al., 2015; Huang *et al.*, 2017; Hardouin *et al.*, 2018; Chen *et al.*, 2020). The orogeny of the Qinling Mountains may have initiated the divergence into independent lineage of *Gekko swinhonis* and *G. konovalovi* (Yan *et al.*, 2010; Chen *et al.*, 2020). Thus, barriers to gene flow produced by complex geological history may be responsible for driving the high level of species diversity in the Qinling Mountains.

These mountains represent a natural boundary between the northern and the southern China, dividing the temperate and subtropical climatic zones in China (Ding *et al.*, 2013), resulting in differentiated terrestrial and freshwater fauna (Li, 1981; Zhang, 2011). The host *R. lagowskii* and gyrodactylids also showed high genetic differentiation and strong geographic structures in East Asia, Europe, and Brazil (Min & Yang, 1986; Bueno-Silva, Boeger & Pie, 2011; Pettersen *et al.*, 2015; Hahn *et al.*, 2015; Hassan *et al.*, 2015; Lumme *et al.*, 2016; Huyse *et al.*, 2017; Xue *et al.*, 2017; Bueno-Silva & Boeger, 2019; Chen *et al.*, 2020). Subpopulations of *M. gonialosae* showed a lack of genetic structure because of the continuous distribution in marine environments (Li *et al.*, 2011). Furthermore, there was a significant positive correlation between genetic differentiation (Fst) and geographic distance, which fit the IBD model in accordance with other studies, suggesting geographic separation (Meng, Li & Qiao, 2014; Yu *et al.*, 2014; Pettersen *et al.*, 2015; Chen *et al.*, 2020). Analyses on the *F. taihangnica* and *Odorrana schmackeri* rejected the IBD model, indicating high level of gene flow and panmixia in these species (Li *et al.*, 2011, 2015; Wang *et al.*, 2013). The genetic differences between lineages of *F. taihangnica* and *G. konovalovi* may reflect the effects of historical isolations caused by tectonic motions and climatic oscillation during the Pleistocene (Wang *et al.*, 2013; Chen *et al.*, 2020). *Rhynchocypris lagowskii* is primarily found on clear cold freshwater from midstream to upstream in East Asia (Zhang & Chen, 1997; Kang, Min & Yang, 2000; Nishida *et al.*, 2015). This specific ecological upstream distribution results in much smaller population sizes and restricts gene flow between host populations, which may have led to the isolation of suprapopulations of *G. konovalovi* (Chen *et al.*, 2020).

A molecular clock estimated the divergence time of *G. konovalovi* was during the Middle Pleistocene in accordance with those for the gyrodactylids *G. corydori*, *Gyrodactylus* spp., *G. teuchis*, *G. arcuatus*, *G. konovalovi*, and *G. gondae* (Bueno-Silva, Boeger & Pie, 2011; Hahn *et al.*, 2015; Lumme *et al.*, 2016; Huyse *et al.*, 2017; Bueno-Silva & Boeger, 2019; Chen *et al.*, 2020). In contrast, the divergence time of *G. salaris* from the Glomma River in Norway was estimated very recent several thousand years during the Holocene after the LGM (Pettersen *et al.*, 2015). The orogeny of the Qinling Mountains may have initiated divergence into the independent lineage of *G. swinhonis* and *G. konovalovi* (Yan *et al.*, 2010; Chen *et al.*, 2020), while the estimated divergence times in the Middle to Late Pleistocene might correspond to the rapid uplift (500–1500 m) of these mountains that were influenced by the Qinghai-Tibet Plateau movement (Zhang & Fang, 2012). The phylogeographic distribution of freshwater fishes was affected by climate fluctuation during the Pleistocene (Gao *et al.*, 2012), and the phylogeographic distribution of *R. oxycephalus* was affected by geological events and Pliocene climate fluctuations (Yu *et al.*, 2014), while, the phylogeographic distribution of *G. konovalovi* was affected by geological events and climate fluctuations during the Pleistocene (Chen *et al.*, 2020). The phylogeography of amphibians species was profoundly influenced by climate fluctuations during the Pleistocene and tectonic changes during the Late Miocene to Late Pleistocene in the Qinling Mountains (Wang *et al.*, 2013; Meng, Li & Qiao, 2014).

Most demographic analyses indicated that the expansion of lineages A and B of *G. konovalovi* began simultaneously, 0.015 Mya after the LGM during the Late Pleistocene, which corresponds to the end of Dali glaciation in the Qinling Mountains. In accordance with findings in *M. gonialosae*, *G. arcuatus*, *G. gondae*, and *G. corydori* in other region (Bueno-Silva, Boeger & Pie, 2011; Li *et al.*, 2011; Lumme *et al.*, 2016; Huyse *et al.*, 2017), while, the suprapopulations of *Gyrodactylus* spp. from *Scleromystax* spp. have expanded in the last 0.25 Mya in Brazil (Bueno-Silva & Boeger, 2019). The Bayesian skyline plot of the lineage C revealed that suprapopulations of *G. konovalovi* expanded, approximately, in the last 15,000 years during the Late Pleistocene, while, the BSP plot of lineages of the suprapopulations of *G. konovalovi* began simultaneously, 0.01 Mya during the Holocene (Chen *et al.*, 2020). Also, this BSP revealed that these suprapopulations were stable between 0.25–0.15 Mya, and then they underwent a decline in population size between 0.15–0.025 Mya, while, previous study of the same parasite underwent sharp contraction between 0.25–0.01 Mya (Chen *et al.*, 2020), this result showed that after the LGM, suprapopulations of *G. konovalovi* expanded along with temperature turning warm, which corresponds to the end of Lushan glaciations in accordance with *F. taihangnica* in the Qinling Mountains (Huang, 1982; Wang *et al.*, 2013). The values from the neutrality test for the lineages A, B, and C were not significant with the positive or negative values (Chen *et al.*, 2020), and the mismatch distribution was multimodal except for lineages A and B, suggesting stability, while the lineage C of *G. konovalovi* distributed in the middle and eastern Qinling Mountains underwent a sharp reduction in the size due to climate drop after the LGM during the Pleistocene and suggested a bottleneck effect (Land, 1988; Chen *et al.*, 2020). A slightly different form of bottleneck can occur if a small group becomes geographically separated from the main population, such as through a founder event, such populations are often small and show increased sensitivity to genetic drift, an increased inbreeding, and relatively low genetic variation (Lynch, Conery & Burger, 1995). Ancient

population bottlenecks or founder effects may have reduced genetic diversity. Therefore, climatic oscillation and tectonic changes that led to vicariance and drainage capture, during the Pleistocene affected the phylogeography of *G. konovalovi* in the Qinling Mountains (Chen *et al.*, 2020).

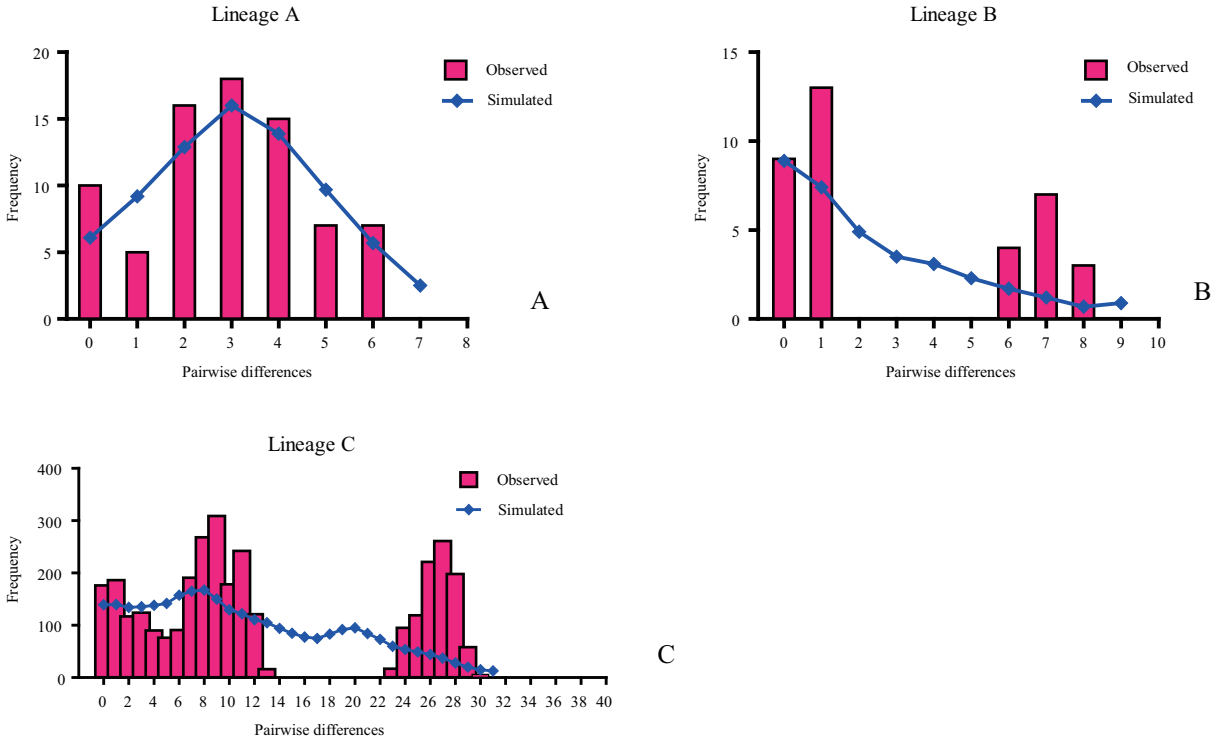

Figure 5. Mismatch distributions for three lineages of *G. konovalovi*. The observed pairwise differences are shown as red bars and the simulated values under the sudden expansion model are indicated by blue solid lines.

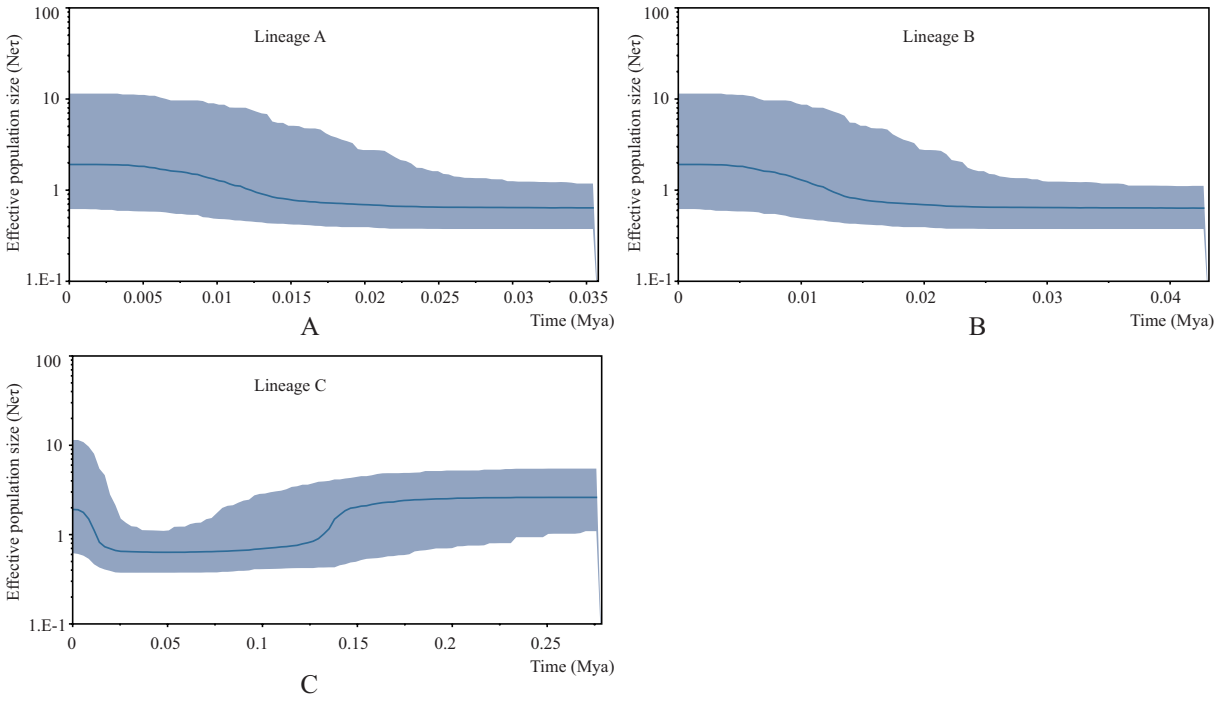

Figure 6. Bayesian skyline plot estimated for the demographic patterns of three lineages of *G. konovalovi*. The X-axis represents time in millions of years, and the Y-axis represents effective population size. The solid line represents the median value of population size, and the dashed lines represent the 95% higher posterior density.

5 Conclusions

The study showed that the tectonic changes and climatic oscillation may have affected distribution pattern of *G. konovalovi* during the Middle to Late Pleistocene, promoting the lineages divergence and influencing the phylogeographic structure of *G. konovalovi* in the Qinling Mountains. After the LGM, lineages A and B have experienced expansions of population size and range during the Late Pleistocene, while the lineage C underwent population contraction during the Middle to Late Pleistocene. Further study employing extensive sampling across larger ranges, more specimens of this parasite, and multiple molecular markers might provide more insight into the phylogeography of *G. konovalovi* across the whole geographical range in the Qinling Mountains.

Funding This work was supported by the National Natural Science Foundation of China (31872203) and the Natural Science Foundation of Shaanxi Province (2017JM3014).

Acknowledgments The authors would like to thank Fangluan Gao (College of Plant Protection, Fujian Agriculture and Forestry University) for assistance with the analysis software. The authors would also like to thank American Journal Experts for editing the manuscript for English language.

References

Albert, J.S., Crampton, W.G.R. 2010. The geography and ecology of diversification in Neotropical freshwaters. *Nature Education Knowledge*, 3(10): 13.

Albert, J.S., Schoolmaster, D.R.J., Tagliacollo, V., Duke-Sylvester, S.M. 2017. Barrier displacement on a neutral landscape: towards a theory of continental biogeography. *Systematic Biology*, 66(2): 167–182. doi: 10.1093/sysbio/syw080.

Avise, J.C. 2000. *Phylogeography: The History and Formation of Species*. Harvard University Press, Cambridge, MA. 447pp.

Avise, J.C., Arnold, J., Ball, R.M., Bermingham, E., Lamb, T., Neigel, J.E., Reeb, C.A., Saunders, N.C. 1987. Intraspecific phylogeography: the mitochondrial DNA bridge between population genetics and systematics. *Annual Review of Ecology and Systematics*, 18: 489–522.

Bakke, T.A., Cable, J., Harris, P.D. 2007. The biology of gyrodactylid monogeneans: the "Russian-doll killers". *Advances in Parasitology*, 64(64): 161–376. doi: 10.1016/S0065-308X(06)64003-7.

Bandelt, H.J., Forster, P., Röhl, A. 1999. Median-joining networks for inferring intraspecific phylogenies. *Molecular Biology and Evolution*, 16(1): 37–48. doi: 10.1093/oxfordjournals.molbev.a026036.

Blasco-Costa, I., Waters, J.M., Poulin, R. 2012. Swimming against the current: genetic structure, host mobility and the drift paradox in trematode parasites. *Molecular Ecology*, 21(1): 207–217. doi: 10.1111/j.1365-294X.2011.05374.x.

Boeger, W.A., Kritsky, D.C., Pie, M.R. 2003. Context of diversification of the viviparous Gyrodactylidae (Platyhelminthes, Monogenoidea). *Zoologica Scripta*, 32(5): 437–448. doi: 10.1046/j.1463-6409.2003.00130.x.

Bowen, B.W., Gaither, M.R., DiBattista, J.D., Iacchei, M., Andrews, K.R., Grant, W.S., Toonen, R.J., Briggs, J.C. 2016. Comparative phylogeography of the ocean planet. *Proceedings of the National Academy of Sciences of the United States of America*, 113(29): 7962–7969. doi: 10.1073/pnas.1602404113.

Brown, W.M., George, M.Jr., Wilson, G.A.C. 1979. Rapid evolution of animal mitochondrial DNA. *Proceedings of the National Academy of Sciences of the United States of America*, 76(4): 1967–1971. doi: 10.1073/pnas.76.4.1967.

Bueno-Silva, M., Boeger, W.A. 2019. Rapid divergence, molecular evolution, and morphological diversification of coastal host-parasite systems from southern Brazil. *Parasitology*, 146(10): 1313–1332. doi: 10.1017/S0031182019000556.

Bueno-Silva, M., Boeger, W.A., Pie, M.R. 2011. Choice matters: incipient speciation in *Gyrodactylus corydori* (Monogenoidea: Gyrodactylidae). *International Journal for Parasitology*, 41(6): 657–667. doi: 10.1016/j.ijpara.2011.01.002.

Chen, T. 2018. Research progress of the biology and taxonomic on parasite *Gyrodactylus* in fish. *Fisheries Science*, 35(5): 707–713. doi: 10.16378/j.cnki.1003-1111.2018.05.021.

Chen, T., Chen, J., Tang, L., Chen, X.N., Yan, J., You, P. 2020. Phylogeography and demographic history of *Gyrodactylus konovalovi* (Monogenoidea: Gyrodactylidae), an ectoparasite on the East Asia Amur minnow (Cyprinidae) in Central China. *Ecology and Evolution*, 10(3): 1454–1468. doi: 10.1002/ece3.6000.

Clayton, D.A. 1982. Replication of animal mitochondrial DNA. *Cell*, 28(4): 693–705. doi: 10.1016/0092-8674(82)90049-6.

Criscione, C.D., Blouin, M.S. 2004. Life cycles shape parasite evolution: comparative population genetics of salmon trematodes. *Evolution*, 58(1): 198–202. doi: 10.1554/03-359.

Darriba, D., Taboada, G.L., Doallo, R., Posada, D. 2012. jModelTest 2: more models, new heuristics and parallel computing. *Nature Methods*, 9(8): 772. doi: 10.1038/nmeth.2109.

Ding, Y.H., Wang, S.W., Zheng, J.Y., Wang, H.J., Yang, X.Q. 2013. *China Climate*. Science Press, Beijing. pp.392–418.

Drummond, A.J., Rambaut, A. 2007. BEAST: Bayesian evolutionary analysis by sampling trees. *BMC Evolutionary Biology*, 7(1): 214. doi: 10.1186/1471-2148-7-214.

Edgar, R.C. 2004. MUSCLE: multiple sequence alignment with high accuracy and high throughput. *Nucleic Acids Research*, 32(5): 1792–1797. doi: 10.1093/nar/gkh340.

Ergens, R. 1976. *Gyrodactylus konovalovi* sp. n. (Gyrodactylidae: Monogenoidea) from *Phoxinus lagowskii* Dybowski. *Folia Parasitologica*, 23(1): 287–289.

Excoffier, L., Lischer, H.E.L. 2010. Arlequin suite ver 3.5: a new series of programs to perform opulation genetics analyses under Linux and Windows. *Molecular Ecology Resources*, 10(3): 564–567. doi: 10.1111/j.1755-0998.2010.02847.x.

Fu, Y.X., Li, W.H. 1993. Statistical tests of neutrality of mutations. *Genetics*, 133(3): 693–709.

Gao, Y., Wang, S.Y., Luo, J., Murphy, R.W., Du, R., Wu, S.F., Zhu, C.L., Li, Y., Poyarkov, A.D., Nguyen, S.N., Luan, P.T., Zhang, Y.P. 2012. Quaternary palaeoenvironmental oscillations drove the evolution of the Eurasian *Carassius auratus* complex (Cypriniformes, Cyprinidae). *Journal of Biogeography*, 39(12): 2264–2278. doi: 10.1111/j.1365-2699.2012.02755.x.

Giles, R.E., Blanc, H., Cann, R.M., Wallace, D.C. 1980. Maternal inheritance of human mitochondrial DNA. *Proceedings of the National Academy of Sciences of the United States of America*, 77(11): 6715–6719. doi: 10.1073/pnas.77.11.6715.

Grant, W.A.S., Bowen, B.W. 1998. Shallow population histories in deep evolutionary lineages of marine fishes: insights from sardines and anchovies and lessons for conservation. *Journal of Heredity*, 89(5): 415–426. doi: 10.1093/jhered/89.5.415.

Hahn, C., Weiss, S.J., Stojanovski, S., Bachmann, L. 2015. Co-speciation of the ectoparasite *Gyrodactylus teuchis* (Monogenea, Platyhelminthes) and its salmonid hosts. *PLoS ONE*, 10(6): e0127340. doi: 10.1371/journal.pone.0127340.

Hall, T.A. 1999. BioEdit: a user-friendly biological sequence alignment editor and analysis program for Windows 95/98/NT. *Nucleic Acids Symposium Series*, 41(41): 95–98.

Hansen, H., Bakke, T.A., Bachmann, L. 2007. Mitochondrial haplotype diversity of *Gyrodactylus thymalli* (Platyhelminthes; Monogenea): extended geographic sampling in United Kingdom, Poland, and Norway reveals further lineages. *Parasitology Research*, 100(6): 1389–1394: doi: 10.1007/s00436-006-0423-5.

Hardouin, E.A., Andreou, D., Zhao, Y.H., Chevret, P., Fletcher, D.H., Britton, J.R., Gozlan, R.E. 2018. Reconciling the biogeography of an invader through recentand historic genetic patterns: the case of topmouth gudgeon *Pseudorasbora parva*. *Biological Invasions*, 20(8): 2157–2171. doi: 10.1007/s10530-018-1693-4.

Harpending, H.C. 1994. Signature of ancient population growth in a low-resolution mitochondrial DNA mismatch distribution. *Human Biology*, 6(4): 591–600.

Harris, P.D., Shinn, A.P., Cable, J., Bakke, T.A. 2004. Nominal species of the genus *Gyrodactylus* von Nordmann 1832 (Monogenea: Gyrodactylidae), with a list of principal host species. *Systematic Parasitology*, 59(1): 1–27. doi: 10.1023/B:SYPA.0000038447.52015.e4.

Hassan, C.M.M., Ishikawa, T., Seki, S., Mahmuda, A. 2015. Genetic population structure of the Aburahaya (*Rhynchocypris lagowskii*) based on mitochondrial DNA sequence. *World Applied Sciences Journal*, 33(7): 1079–1088. doi: 10.5829/idosi.wasj.2015.33.07.94254.

Hewitt, G.M. 1996. Some genetic consequences of ice ages, and their role in divergence and speciation. *Biological Journal of the Linnean Society*, 58(3): 247–276.

Higuchi, F., Watanabe, K. 2005. Genetic diversity and hybridization in the cyprinid, *Rhynchocypris lagowskii steindachneri*, from Yokohama, central Honshu, Japan. *Japanese Journal of Ichthyology*, 52(1): 41–46.

Huang, P.H. 1982. Quaternary climatic changes in China and problem of Lushan glaciation remnants. *Journal of Glaciology and Geocryology*, 4(3): 1–14.

Huang, Y. 2012. *Molecular Phylogenetics*. Science Press, Beijing. pp. 7–8.

Huang, Z.S., Yu, F.L., Gong, H.S., Song, Y.L., Zeng, Z.G., Zhang, Q. 2017. Phylogeographical structure and demographic expansion in the endemic alpine stream salamander (Hynobiidae: *Batrachuperus*) of the Qinling Mountains. *Scientific Reports*, 7(1871): 1–13. doi: 10.1038/s41598-017-01799-w.

Hunter, M.L.Jr., Gibbs, J.P. 2006. *Fundamentals of Conservation Biology, 3rd Edition*. Blackwell Publishing, Oxford. 516pp.

Huyse, T., Buchmann, K., Littlewood, D.T.J. 2008. The mitochondrial genome of *Gyrodactylus derjavinoides* (Platyhelminthes: Monogenea) - a mitogenomic approach for *Gyrodactylus* species and strain identification. *Gene*, 417(1–2): 27–34. doi: 10.1016/j.gene.2008.03.008.

Huyse, T., Oeyen, M., Larmuseau, M.H.D., Volckaert, F.A.M. 2017. Co-phylogeographic study of the flatworm *Gyrodactylus gondae* and its goby host *Pomatoschistus minutus*. *Parasitology International*, 66(2): 119–125. doi: 10.1016/j.parint.2016.12.008.

Kang, Y.J., Min, M.K., Yang, S.Y. 2000. Reproductive isolation between *Moroco oxycephalus* and *M. lagowskii* (Pisces; Cyprinidae) in Korea. *Korean Journal of Biological Sciences*, 4(2): 109–115. doi: 10.1080/12265071.2000.9647533.

Lande, R. 1988. Genetics and demography in biological conservation. *Science*, 241(4872): 1455–1460. doi: 10.1126/science.3420403.

Li, M., Shi, S.F., Brown, C.L., Yang, T.B. 2011. Phylogeographical pattern of *Mazocraeoides gonialosae* (Monogenea, Mazocraeidae) on the dotted gizzard shad, *Konosirus punctatu*s, along the coast of China. *International Journal for Parasitology*, 41(12): 1263–1272. doi: 10.1016/j.ijpara.2011.07.012.

Li, S.Z. 1981. *Studies on Zoogeographical Divisions for Freshwater Fishes of China*. Science Press, Beijing. 292pp.

Li, Y.M., Wu, X.Y., Zhang, H.B., Yan, P., Xue, H., Wu, X.B. 2015. Vicariance and its impact on the molecular ecology of a Chinese ranid frog species-complex (*Odorrana schmackeri*, Ranidae). *PLoS ONE*, 10(9): e0138757. doi: 10.1371/journal.pone.0138757.

Librado, P., Rozas, J. 2009. DnaSP v5: a software for comprehensive analysis of DNA polymorphism data. *Bioinformatics*, 25(11): 1451–1452. doi: 10.1093/bioinformatics/btp187.

Liu, H.X., Li, Y., Liu, X.L., Xiong, D.M., Wang, L.X., Zou, G.W., Wei, Q.W. 2015. Phylogeographic structure of *Brachymystax lenok tsinlingensis* (Salmonidae) populations in the Qinling Mountains, Shaanxi, based on mtDNA control region. *Mitochondrial DNA*, 26(4): 532–537. doi: 10.3109/19401736.2013.865168.

Llewellyn, J. 1984. The biology of *Isancistrum subulatae* n. sp. a monogenean parasitic on the squid, *Alloteuthis subulata*, at Plymouth. *Journal of the Marine Biological Association of the UK*, 64(2): 285–302.

Lumme, J., Mäkinen, H., Ermolenko, A.V., Gregg, J.L., Ziętara, M.S. 2016. Displaced phylogeographic signals from *Gyrodactylus arcuatus,* a parasite of the three-spined stickleback *Gasterosteus aculeatus*, suggest freshwater glacial refugia in Europe. *International Journal for Parasitology*, 46(9): 545–554. doi: 10.1016/j.ijpara.2016.03.008.

Lumme, J., Ziętara, M.S., Lebedeva, D. 2017. Ancient and modern genome shuffling: reticulate mito-nuclear phylogeny of four related allopatric species of *Gyrodactylus* von Nordmann, 1832 (Monogenea: Gyrodactylidae), ectoparasites on the Eurasian minnow *Phoxinus phoxinus* (L.) (Cyprinidae). *Systematic Parasitology*, 94(2): 183–200. doi: 10.1007/s11230-016-9696-y.

Lynch, M., Conery, J., Burger, R. 1995. Mutation accumulation and the extinction of small populations. *The American Naturalist*, 146(4): 489–518.

Meinilä, M., Kuusela, J., Ziętara, M.S., Lumme, J. 2002. Primers for amplifying approximately 820 bp of highly polymorphic mitochondrial COI gene of *Gyrodactylus salaris*. *Hereditas*, 137(1): 72–74. doi: 10.1034/j.1601-5223.2002.1370110.x.

Meinilä, M., Kuusela, J., Ziętara, M.S., Lumme, J. 2004. Initial steps of speciation by geographic isolation and host switch in salmonid pathogen *Gyrodactylus salaris* (Monogenea: Gyrodactylidae). *International Journal for Parasitology*, 34(4): 515–526. doi: 10.1016/j.ijpara.2003.12.002.

Meng, H.Z., Li, X.C., Qiao, P.H. 2014. Population structure, historical biogeography and demographic history of the Alpine toad *Scutiger ningshanensis* in the Tsinling Mountains of Central China. *PLoS ONE*, 9(6): e100729. doi: 10.1371/journal.pone.0100729.

Mieszkowska, A., Górniak, M., Jurczak-kurek, A., Ziętara, M.S. 2018. Revision of *Gyrodactylus salaris* phylogeny inspired by new evidence for Eemian crossing between lineages living on grayling in Baltic and White sea basins. *Peerj*, 6: e5167. doi: 10.7717/peerj.5167.

Mills, L.S. 2007. *Conservation of Wildlife Populations: Demography, Genetics, and Management*. Blackwell Publishing, Oxford. 342pp.

Min, M.S., Yang, S.Y. 1986. Classification, distribution and geographic variation of two species of the genus *Moroco* in Korea. *Korean Journal of Systematic Zoology*, 21: 63–78.

Nishida, K., Koizumi, N., Satoh, T., Senga, Y., Takemura, T., Watabe, K., Mori, A. 2015. Influence of the domestic alien fish *Rhynchocypris oxycephalus*, invasion on the distribution of the closely related native fish *R. lagowskii*, in the Tama River Basin, Japan. *Landscape & Ecological Engineering*, 11(1): 169–176. doi: 10.1007/s11355-014-0257-8.

Paetow, L., Cone, D.K., Huyse, T., Mclaughlin, J.D., Marcogliese, D.J. 2009. Morphology and molecular taxonomy of *Gyrodactylus jennyae* n. sp. (Monogenea) from tadpoles of captive *Rana catesbeiana* Shaw (*Anura*), with a review of the species of *Gyrodactylus* Nordmann, 1832 parasitising amphibians. *Systematic Parasitology*, 73(3): 219–227. doi: 10.1007/s11230-009-9183-9.

Pettersen, R.A., Mo, T.A., Hansen, H., Vøllestad, L.A. 2015. Genetic population structure of *Gyrodactylus thymalli* (Monogenea) in a large Norwegian river system. *Parasitology*, 142(14): 1693–1702. doi: 10.1017/S003118201500133X.

Rambaut, A. 2014. FigTree v1.4.2, a graphical viewer of phylogenetic trees. Available from http://tree.bio.ed.ac.uk/software/figtree/ (accessed 5 April 2020).

Rambaut, A., Drummond, A.J., Xie, D., Baele, G., Suchard, M.A. 2018. Posterior summarization in bayesian phylogenetics using Tracer 1.7. *Systematic Biology*, 67(5): 901–904. doi: 10.1093/sysbio/syy032.

Rand, D.M., Kann, L.M. 1998. Mutation and selection at silent and replacement sites in the evolution of animal mitochondrial DNA. *Genetica*, 102: 393–407. doi: 10.1023/A:1017006118852.

Ronquist, F., Huelsenbeck, J.P. 2003. MrBayes 3: Bayesian phylogenetic inference under mixed models. *Bioinformatics*, 19(12): 1572–1574. doi: 10.1093/bioinformatics/btg180.

Rowe, K.C., Heske, E.J., Brown, P.W., Paige, K.N. 2004. Surviving the ice: northern refugia and postglacial colonization. *Proceedings of the National Academy of Sciences of the United States of America*, 101(28): 10355–10359. doi: 10.1073/pnas.0401338101.

Sakai, H., Ueda, T., Yokoyama, R., Safronov, S.N., Goto, A. 2014. Genetic structure and phylogeography of northern Far East pond minnows, *Rhynchocypris perenurus sachalinensis* and *R. p. mantschuricus* (Pisces, Cyprinidae), inferred from mitochondrial DNA sequences. *Biogeography*, 16: 87–109.

Schneider, C.J., Cunningham, M., Moritz, C. 1998. Comparative phylogeography and the history of endemic vertebrates in the wet tropics rainforests of Australia. *Molecular Ecology*, 7(4): 487–498. doi: 10.1046/j1365-294x.1998.00334.x.

Slatkin, M. 1993. Isolation by distance in equilibrium and non-equilibrium populations. *Evolution*, 47(1): 264–279. doi: 10.1111/j.1558-5646.1993.tb01215.x.

Stamatakis, A., Ludwig, T., Meier, H. 2005. RAxML-III: a fast program for maximum likelihood-based inference of large phylogenetic trees. *Bioinformatics*, 21(4): 456–463. doi: 10.1093/bioinformatics/bti191.

Swofford, D.L. 2002. PAUP*. Phylogenetic Analyses Using Parsimony (*and other methods), Version 4.0b10. Sinauer Associates, Sunderland, MA.

Tajima, F. 1989. Statistical method for testing the neutral mutation hypothesis by DNA polymorphism. *Genetics*, 123(3): 585–595.

Tamura, K., Stecher, G., Peterson, D., Filipski, A., Kumar, S. 2013. MEGA6: molecular evolutionary genetics analysis version 6.0. *Molecular Biology and Evolution*, 30(12): 2725–2729. doi: 10.1093/molbev/mst197.

Vanhove, M.M.P., Tessens, B., Schoelinck, C., Jondelius, U., Littlewood, D.T.J., Artois, T., Huyse, T. 2013. Problematic barcoding in flatworms: a case-study on monogeneans and rhabdocoels (Platyhelminthes). *Zookeys*, 365(365): 355–379. doi: 10.3897/zookeys.365.5776.

Wang, B., Jiang, J.P., Xie, F., Li, C. 2012. Postglacial colonization of the Qinling Mountains: phylogeography of the Swelled Vent frog (*Feirana quadranus*). *PLoS ONE*, 7(7): e41579. doi: 10.1371/journal.pone.0041579.

Wang, B., Jiang, J.P., Xie, F., Li, C. 2013. Phylogeographic patterns of mtDNA variation revealed multiple glacial refugia for the frog species *Feirana taihangnica* endemic to the Qinling Mountains. *Journal of Molecular Evolution*, 76(3): 112–128: doi: 10.1007/s00239-013-9544-5.

Wu, B.H., Lang, S., Wang, W.J. 2000. *Fauna Sinica: Platyhelminthes: Monogenea.* Science Press, Beijing. pp. 583–616.

Wu, S.G., Wang, G.T., Xi, B.W., Xiong, F., Liu, T., Nie, P. 2009. Population genetic structure of the parasitic nematode *Camallanus cotti* inferred from DNA sequences of ITS1 rDNA and the mitochondrial COI gene. *Veterinary Parasitology*, 164(2–4): 248–256. doi: 10.1016/j.vetpar.2009.04.030.

Xue, Z., Zhang, Y.Y., Lin, M.S., Sun, S.M., Gao, W.F., Wang, W. 2017. Effects of habitat fragmentation on the population genetic diversity of the Amur minnow (*Phoxinus lagowskii*). *Mitochondrial DNA Part-B Resources*, 2(1): 331–336. doi: 10.1080/23802359.2017.1331319.

Yan, J., Wang, Q.X., Chang, Q., Ji, X., Zhou, K.Y. 2010. The divergence of two independent lineages of an endemic Chinese gecko, *Gekko swinhonis*, launched by the Qinling orogenic belt. *Molecular Ecology*, 19(12): 2490–2500. doi: 10.1111/j.1365-294X.2010.04660.x.

Ye, F., Easy, R.H., King, S.D., Cone, D.K., You, P. 2017. Comparative analyses within *Gyrodactylus* (Platyhelminthes: Monogenea) mitochondrial genomes and conserved polymerase chain reaction primers for gyrodactylid mitochondrial DNA. *Journal of Fish Diseases*, 40(4): 541–555. doi: 10.1111/jfd.12539.

You, P., King, S.D., Ye, F., Cone, D.K. 2014. *Paragyrodactylus variegatus* n. sp. (Gyrodactylidae) from *Homatula variegata* (Dabry De Thiersant, 1874) (Nemacheilidae) in Central China. *Journal of Parasitology*, 100(3): 350–355. doi: 10.1645/13-257.1.

Yu, D., Chen, M., Tang, Q.Y., Li, X.J., Liu, H.Z. 2014. Geological events and Pliocene climate fluctuations explain the phylogeographical pattern of the cold water fish *Rhynchocypris oxycephalus* (Cypriniformes: Cyprinidae) in China. *BMC Evolutionary Biology*, 14: 225. doi: 10.1186/s12862-014-0225-9.

Yue, P.Q., Chen, Y.Y. 1998. *Endangered in China Red Data Book of Endangered Animals – Pisces*. Science Press, Beijing. 247pp.

Zhang, E., Chen, Y.Y. 1997. Fish fauna in northeastern Jiangxi province with a discussion on the zoogeographical division of East China. *Acta Hydrobiologica Sinica*, 21(3): 254–261.

Zhang, L.S., Fang, X.Q. 2012. *Palaeogeography of China: Formation of China's Natural Environment*. Science Press, Beijing. pp. 237–247.

Zhang, R.Z. 2011. *Zoogeography of China*. Science Press, Beijing. pp. 59–65.

Ziętara, M.S., Lumme, J. 2002. Speciation by host switch and adaptive radiation in a fish parasite genus *Gyrodactylus* (Monogenea, Gyrodactylidae). *Evolution*, 56(12): 2445–2458. doi: 10.1111/j.0014-3820.2002.tb00170.x.